Tetrahedron 66 (2010) 3553–3563

Contents lists available at ScienceDirect

Tetrahedron

journal homepage: www.elsevier.com/locate/tet

Novel C_3-symmetrical triphenylbenzene-based organogelators with different linkers between phenyl ring and alkyl chain

Yabing He, Zheng Bian *, Chuanqing Kang, Yanqin Cheng, Lianxun Gao *

State Key Laboratory of Polymer Physics and Chemistry, Changchun Institute of Applied Chemistry, Chinese Academy of Sciences, Graduate School of Chinese Academy of Sciences, Changchun 130022, China

ARTICLE INFO

Article history:
Received 24 September 2009
Received in revised form 22 February 2010
Accepted 26 February 2010
Available online 10 March 2010

ABSTRACT

A new family of 1,3,5-triphenylbenzene-based organogelators with approximately identical side chain length have been synthesized and fully characterized. The molecular aggregation can be promoted by hydrogen-bonding and van der Waals interaction. The magnitudes of hydrogen bonding interactions between the linkers on the triphenylbenzene cores are qualitatively in the order of –CONHNHCO–, –NHCONH–>–NHCO–>–CONH–>–NHCSNH–, consequently resulting in different gelation behaviors. The sol-gel transitions of gels **3** and **4** in toluene are thermodynamically reversible, while the formations of gels **2** and **5** in dioxane are kinetically controlled. The urea-based gel **2** can selectively recognize F^- ion.

1. Introduction

In the past decade, the introduction of the beautiful C_3-symmetry into molecular structure has acquired much interest from the supramolecular chemists.[1] Especially, many C_3-symmetrical low molecular weight organo- or hydrogelators (LMWGs) have been designed and synthesized successfully.[2–11] In common, the *cis*,*cis*-1,3,5-cylcohexane triamide or triamidobenzene cores are used as the gelating scaffolds. The parallel orientation of the hydrogen bond-based units on the cores provides strong uniaxial intermolecular interactions affording 1 D self-assembly perpendicular to the plane of the molecule. By further extension toward the outside from the core, a broad scope of functionalities can be introduced.[2–8] Furthermore, the research for the tuning of mechanical or thermal properties of the gels, the scope of gelated solvents and morphology of the gels is elementary in the field of gel chemistry.[3] A better understanding of the structure-property relationship of a gelator is of great interest and importance. Ben L. Feringa et al.[10] and Masamichi Yamanaka et al.[11] ever systematically developed the C_3-symmetric organogelator with a broad structural variation. Interestingly, the intermolecular interactions strongly depend on the nature of the core units, the type of hydrogen-bonding units and the side groups, and consequently there are large differences in aggregation properties, thermal stability, and morphology between the various compounds.

Recently, Lu Ran et al. reported a series of 1,3,5-triphenylbenzene derivatives with long alkoxy sidechains whose accumulation structures may be tuned by the chain length and the number of chains.[9] Different from the rigid benzene core, a triphenylbenzene molecule possesses the labile conformation, and a propeller-like one is energetically favorable. In particular, the C_2-symmetrical *para*-terphenylen-1,4″-ylenebis(dodecanamide) can self-assemble into the nanotube structure, but is almost insoluble in any solvent at room temperature.[12] The π–π interaction between rigid terphenylene segments and the intermolecular hydrogen bonding between amido units have a synergistic effect on the formation of extremely stable aggregation. So the exploration for the structurally similar C_3-symmetrical triphenylbenzene-centered molecules seems to be very interesting. In this paper, we describe the aggregation behaviors of a new family of triphenylbenzene-centered molecules **1**–**6** with approximately identical side chain length. Our interest is focused on the effect of different hydrogen bond-based linkers between phenyl ring and long alkyl chain on gelation properties (Scheme 1).

2. Results and discussion

2.1. Synthesis

A family of triphenylbenzene-centered molecules **1**–**6** were prepared according to the procedures described in Scheme 2. Tetrachlorosilane catalyzed condensation of *p*-nitroacetophenone in dry ethanol gave 1,3,5-tri(4-nitrophenyl)-benzene. Reduction of the nitro group proceeded in the presence of hydrazine with Pd/C as catalyst in THF under reflux and provided triamino **7**. Trithiourea **1** and triurea **2** were obtained by the reaction of triamino **7** with dodecyl thioisocyanate or isocyanate in dry THF, respectively.

* Corresponding authors. Tel.: +86 431 85262265; fax: +86 431 85697831; e-mail addresses: bianzh@ciac.jl.cn (Z. Bian), lxgao@ciac.jl.cn (L. Gao).

0040-4020/$ – see front matter © 2010 Elsevier Ltd. All rights reserved.
doi:10.1016/j.tet.2010.02.094

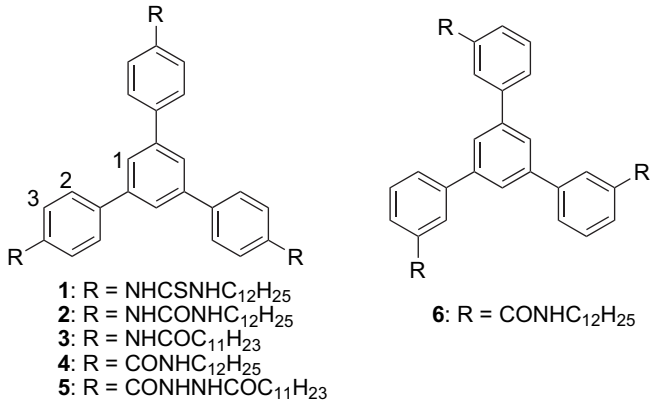

Scheme 1.

Treating triamino **7** with dodecanoyl chloride in dry THF using triethylamine as base gave triamide **3**. Suzuki cross-coupling of 1,3,5-tribromobenzene and *p*-methoxycarbonylphenyl boronic acid in the presence of $Pd(PPh_3)_4$ as catalyst and Na_2CO_3 as base followed by basic hydrolysis provided **8**. Likewise, **9** was obtained from 1,3,5-tribromobenzene and *m*-methoxycarbonylphenyl boronic acid. Heating **8** in $SOCl_2$ to give 1,3,5-tri(*p*-chlorocarbonylphenyl)benzene followed by reaction with dodecan-1-amine or dodecanehydrazide provided the investigated derivatives **4** or **5**, respectively. Triamide **6** was prepared as described for **4**, starting from **9** and dodecan-1-amine. The chemical structures of all compounds were confirmed by ^1H NMR, ^{13}C NMR, FTIR, ESI-MS, and elemental analysis.

2.2. Gel test

All compounds **1**–**6** were first studied with regard to their gelation behavior in various solvents using a test tube inversion method (Fig. 1). The organogelation properties of **1**–**6** are listed in Table 1. Trithiourea **1** has poor organogelation ability and only at −10 °C forms the gels in aromatic solvents such as toluene, xylene, mesitylene, possibly due to weak hydrogen bonding interactions between thiourea groups. However, triurea **2** forms the gels in chloroform and cyclic ether solvents such as THF and dioxane with low critical gel concentration (CGC). When the urea groups are replaced by the amide groups, triamide **3** exhibits a high CGC value in chloroform, but it shows good gelation ability in aromatic solvents. In contrast, triurea **2** is insoluble in aromatic solvents. When the linking mode of amide is inverted, the resulting derivative **4** has

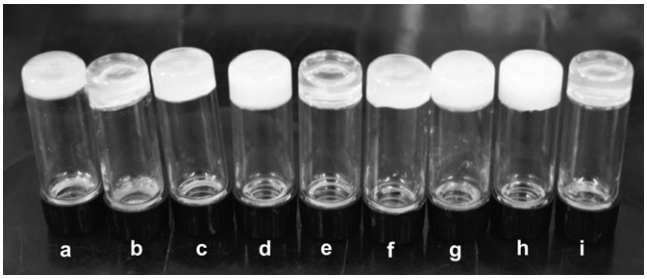

Figure 1. Gel photographs. (a) gel **3** in chloroform (20 mg mL^{-1}), (b) gel **3**in toluene (20 mg mL^{-1}), (c) gel **5** in THF (6 mg mL^{-1}), (d) gel **5**in dioxane(4 mg mL^{-1}), (e) gel **2** in chloroform (3 mg mL^{-1}), (f) gel **2** in THF (10 mg mL^{-1}), (g) gel **2** in dioxane (1.5 mg mL^{-1}), (h) gel **4** in ethyl acetate (5 mg mL^{-1}), (i) gel **4** in toluene (10 mg mL^{-1}).

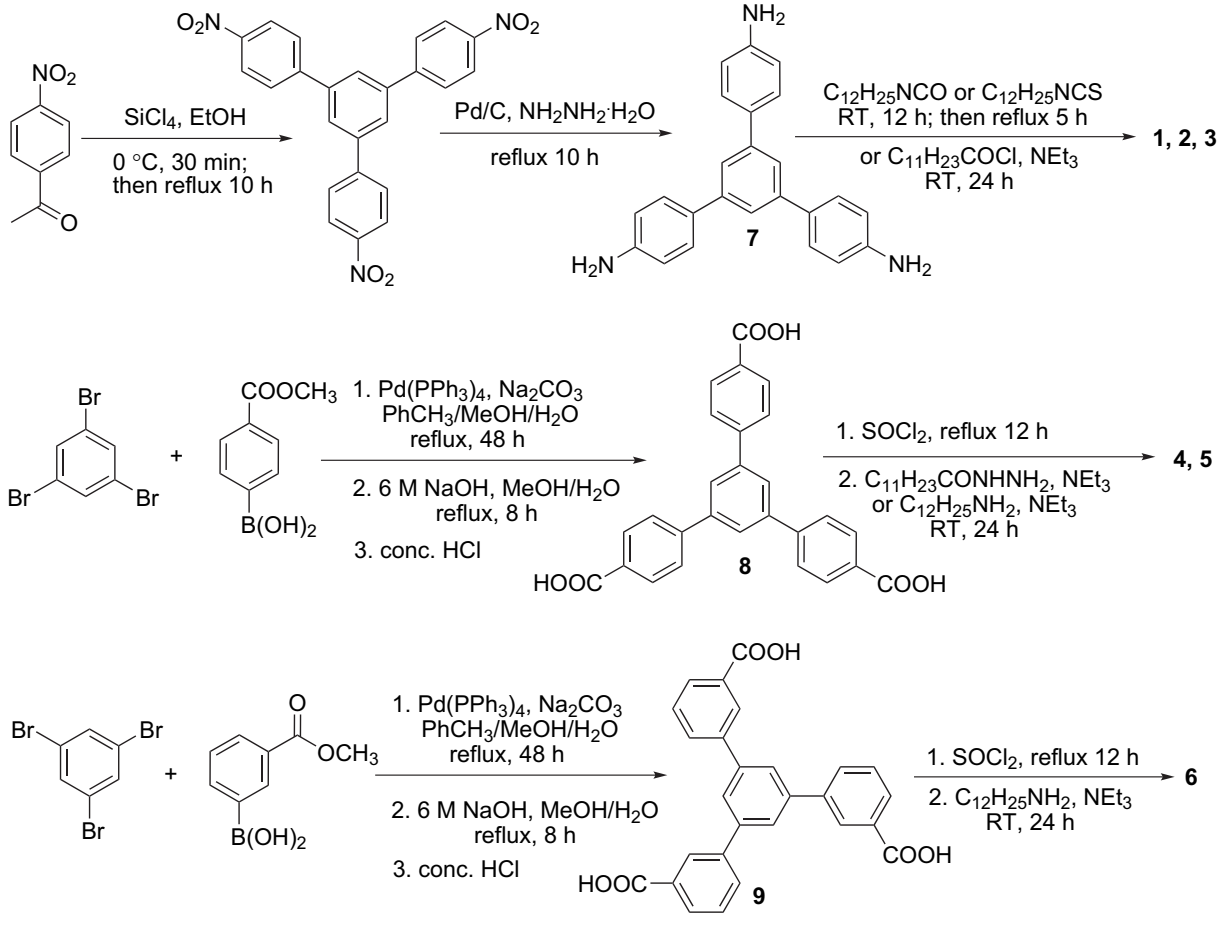

Scheme 2. The synthetic routes to the compounds **1**–**6**.

Table 1
Gelation properties of **1**–**6**[a]

solvent	1	2	3	4	5	6
$CHCl_3$	S	G (2.0)	G (20)	S	WG	S
THF	S	G (3.0)	S	S	G (5.0)	S
Dioxane	S	G (1.0)	S	S	G (2.5)	S
EtOAc	P	I	P	G (5.0)	I	P
acetone	P	I	P	P	I	P
Acetonitrile	P	P	P	P	I	P
Toluene	VS	I	G (5.0)	G (10)	I	P
Xylene	VS	I	G (5.0)	G (10)	I	P
Mesitylene	VS	I	G (5.0)	G (10)	I	P
n-Hexane	I	I	I	I	I	I
DMF	S	P	S	S	S	S

[a] S=solution, P=precipitation, G=gelation, I=insoluble, VS=viscous solution, WG=weak gel. The values in the brackets denote the CGC values (mg mL^{-1}) of gelators at 25 °C.

relatively poor gelation ability in aromatic solvents, but it can gelate ethyl acetate. With further increase of the number of amide bond, **5** loses the gelation ability in aromatic solvents, but can gelate THF and dioxane. When the linking position of amide is changed from *p*- to *m*-position of the phenyl ring, **6** completely loses gelation ability in tested solvents. According to Masamichi's results,[11] the *m*-substituted phenyl ring region could not be flexible enough, and consequently, it is difficult for **6** to form the effective 1 D aggregate. Evidently, triurea **2** is the best organogelator for polar solvents, and triamide **3** for aromatic solvents.

The gelation time depends on the tested solvents. In general, the formation of a gel need one minute in aromatic solvents, three minutes in cyclic ether solvents and ethyl acetate, and at least 15 min in chloroform. The gelation also depends on the cooling rate. When the hot solutions in dioxane are slowly cooled to room temperature (1 °C min^{-1}), **2** and **5** do not form gel but precipitate. The formed gels are stable at room temperature for months. It should be noted that gels **2** and **3** in chloroform can be damaged by modest shake with hand.

The gel test also shows that **2**–**5** are moderately soluble in many solvents, suggesting that the intermolecular interaction is weak in contrast to that of *para*-terphenylen-1,4″-ylenebis(dodecanamide) and there couldn't exist a synergistic effect to promote extremely steady aggregation.[12]

2.3. FT-IR study

IR spectroscopy is a powerful tool for studying hydrogen bonding and van der Waals forces. Figure 2 shows FT-IR spectra of **4** in THF solution and xerogel. In a THF solution, the typical absorption bands, characteristic of the non-hydrogen bonded amide groups, are observed around 3455 cm^{-1} (ν_{N-H}), 1654 cm^{-1} ($\nu_{C=O}$) and 1527 cm^{-1} (δ_{N-H}). In contrast, the IR peaks of the xerogel from ethyl acetate appear around 3298 cm^{-1} (ν_{N-H}), 1636 cm^{-1} ($\nu_{C=O}$) and 1545 cm^{-1} (δ_{N-H}) due to hydrogen bonded amide groups. These results indicate that one of the driving forces for organogelation is intermolecular hydrogen bonding between the amide groups.

In addition, the absorption bands arising from the antisymmetric (νas_{C-H}) and symmetric (νs_{C-H}) stretching vibrations of the alkyl chains are observed at 2928 cm^{-1} and 2856 cm^{-1} in THF solution, indicating the presence of a *gauche*-form alkyl chain. But these IR bands of the xerogel appearing at 2924 cm^{-1} (νas_{C-H}) and 2852 cm^{-1} (νs_{C-H}) correspond to the alkyl chain in the all-*trans* form.[13] Such low wavenumber shifts of the IR bands of νas_{C-H} and νs_{C-H} demonstrate the decreased mobility of the alkyl chain. Consequently, it is clear that the van der Waals interaction between the alkyl chains is present in the gel.

Moreover, for all xerogels **4** prepared from different solvents, the peaks arising from the hydrogen-bonded amide are independent on solvents and are consistent with those in the solid states, indicating that the nature of intermolecular hydrogen bonding in the solid and gel is the same, and does not significantly depend on the gelling solvents.

The peaks of other compounds assigned to hydrogen-bonded amides and alkyl chains are summarized in Table 2.

Table 2
FT-IR data of xerogels **2**–**5** from different solvents (cm^{-1})

Xerogel	ν_{N-H}	$\nu_{C=O}$	δ_{N-H}	νas_{C-H}	νs_{C-H}
2 ($CHCl_3$)	3324	1645	1555	2923	2852
2 (THF)	3323	1643	1555	2922	2852
2 (Dioxane)	3333	1644	1559	2925	2854
3 ($CHCl_3$)	3292	1660	1524	2923	2852
3 (Toluene)	3291	1659	1526	2923	2852
4 (EtOAc)	3299	1635	1544	2923	2852
4 ($CHCl_3$/*n*-hexane)	3299	1636	1545	2924	2852
4 (THF/*n*-hexane)	3299	1635	1544	2923	2852
4 (Toluene)	3300	1636	1544	2923	2852
5 (THF)	3205	1601	1471	2922	2853
5 (Dioxane)	3208	1601	1471	2924	2853

For xerogel **2** from THF, the N–H and C=O stretching and N–H bending vibration modes of urea groups are located at 3323, 1643, and 1555 cm^{-1}, characteristic of hydrogen-bonding mode of stabilization of aggregates of urea derivatives.[14] The xerogels **3** and **5** also have the similar behaviors. The absorption bands of **3** and **5** arising from N–H and C=O stretching and N–H bending vibration are observed at 3292, 1660, 1524 cm^{-1} and 3205, 1601, 1471 cm^{-1}, respectively, indicating the hydrogen bonding interactions between amide groups.[15]

2.4. NMR investigation

NMR technique is employed to probe the assembly process. Due to poor solubility of **2** and **5** in $CDCl_3$, only **3** and **4** were characterized by concentration-dependent (CD) and temperature-dependent (TD) NMR methods. In ^1H NMR spectra of **4** at 27 °C, the peaks assigned to amide shift downfield with increasing concentration (Fig. 3a), derived from multimolecular aggregation. This is also supported by TD-NMR experiments. With increasing temperature, the peaks assigned to amide shift upfield (Fig. 3b). Moreover, these signal peaks become broader at higher concentration or lower temperature. All these observations point toward the intermolecular aggregation of **4** in solution by hydrogen bonding interaction. Compound **3** also exhibits the similar properties (Fig. 3c–d). However, the proton signals assigned to the triphenylbenzene unit don't exhibit a significant shift, suggesting that the intermolecular π–π interactions are relatively weak.

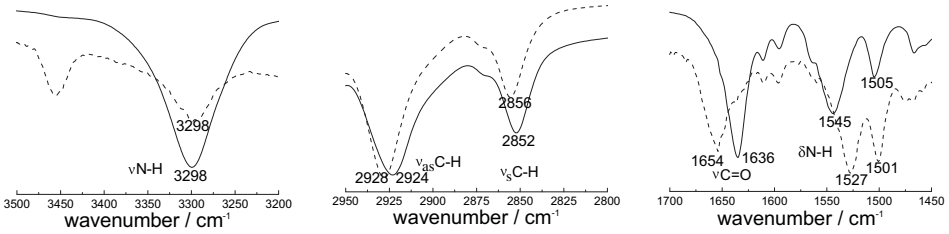

Figure 2. FT-IR spectra of **4** in THF solution (1.0×10^{-2} M) (dashed line) and xerogel from ethyl acetate (solid line).

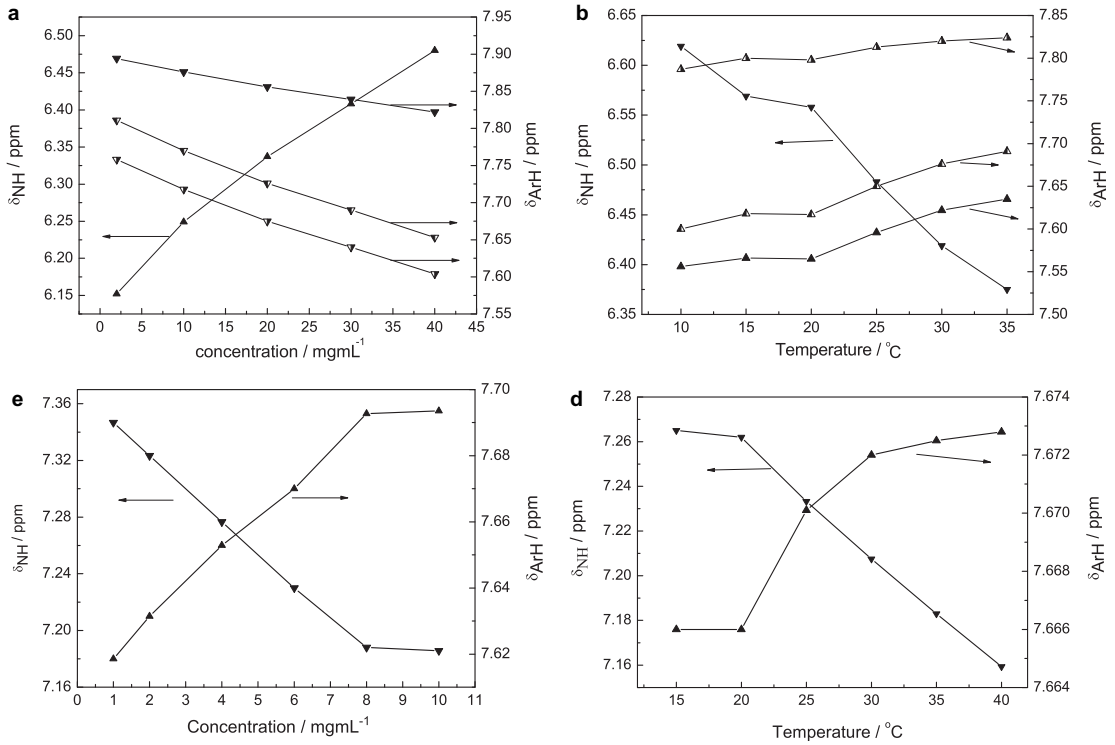

Figure 3. Concentration and temperature dependence of chemical shifts of **4** (a and b) and **3** (c and d).

According to FT-IR and NMR analyses, the aggregation of the gelator molecules is promoted mainly by hydrogen bonding and van de Waals interaction. Furthermore, referred to abovementioned gel test, it can be seen that the magnitudes of intermolecular hydrogen bonding inter-actions are qualitatively in the order of –CONHNHCO–, –NHCONH–>–NHCO–>–CONH–>–NHCSNH–.

2.5. DSC analyses

The thermal properties of the gels were investigated by differential scanning calorimetry (DSC). Representative sets of thermograms with gels **2** in dioxane, **3** in toluene, **4** in toluene, and **5** in dioxane are shown in Figure 4. The DSC curves of gels **3** and **4** in toluene clearly exhibit very broad endothermic transitions upon

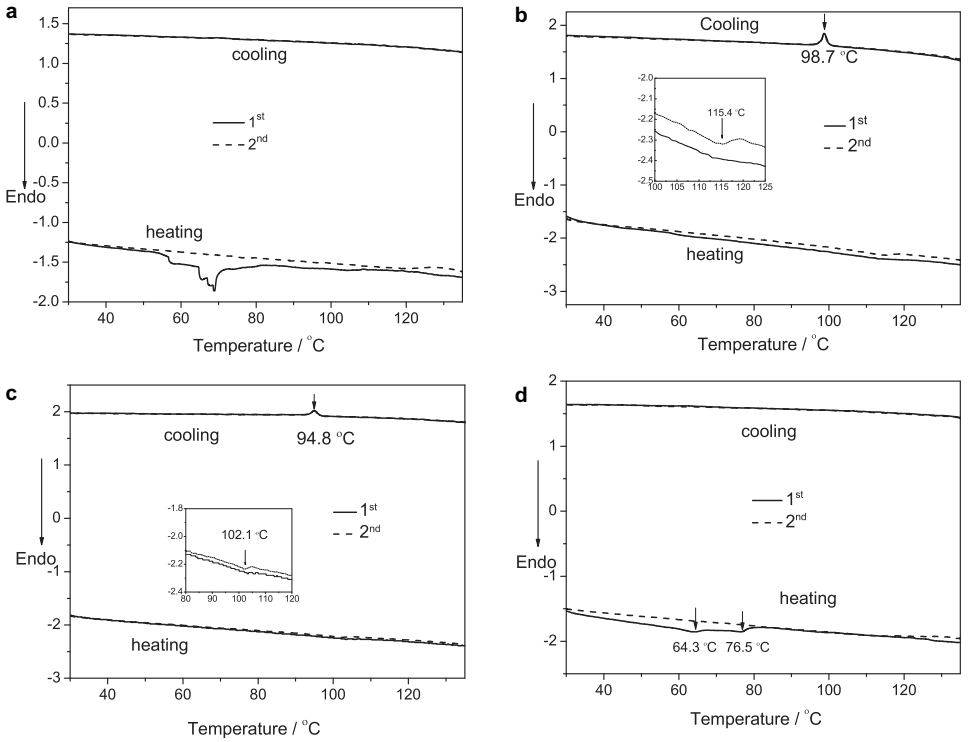

Figure 4. DSC curves of gels **2** in dioxane (a), **3** in toluene (b), **4** in toluene (c), and **5** in dioxane (d) with a concentration of 1.52×10^{-3} mol L^{-1}, 2.23×10^{-2} mol L^{-1}, 1.06×10^{-2} mol L^{-1}, and 3.9×10^{-3} mol L^{-1}, respectively. Heating and cooling rate, 2 °C min^{-1}.

melting with the maxima at 115.4 °C and 102.1 °C, respectively, characteristic of the supramolecular aggregates. When the mixtures are cooled down, the sharp exothermic transitions are observed with maxima at 98.7 °C and 94.8 °C, respectively. Repeated cycle shows similar transition behaviors. These phenomena suggest that the sol-gel transitions of gels **3** and **4** in toluene are thermodynamically reversible.

The DSC curves of gels **2** and **5** in dioxane also show broad endothermic transitions on heating, but no evident exothermic transition on cooling in the first heating and cooling cycle. Particularly, the endothermic transitions disappear in the second cycle. Combined with above-mentioned experimental results that **2** and **5** form precipitate on cooling slowly, a conclusion can be drawn that the formations of gels **2** and **5** in dioxane are kinetically controlled.

2.6. Microscopy

It is well known that a supramolecular gel is often formed by self-assembled nanofibers. The scanning electronic microscopy

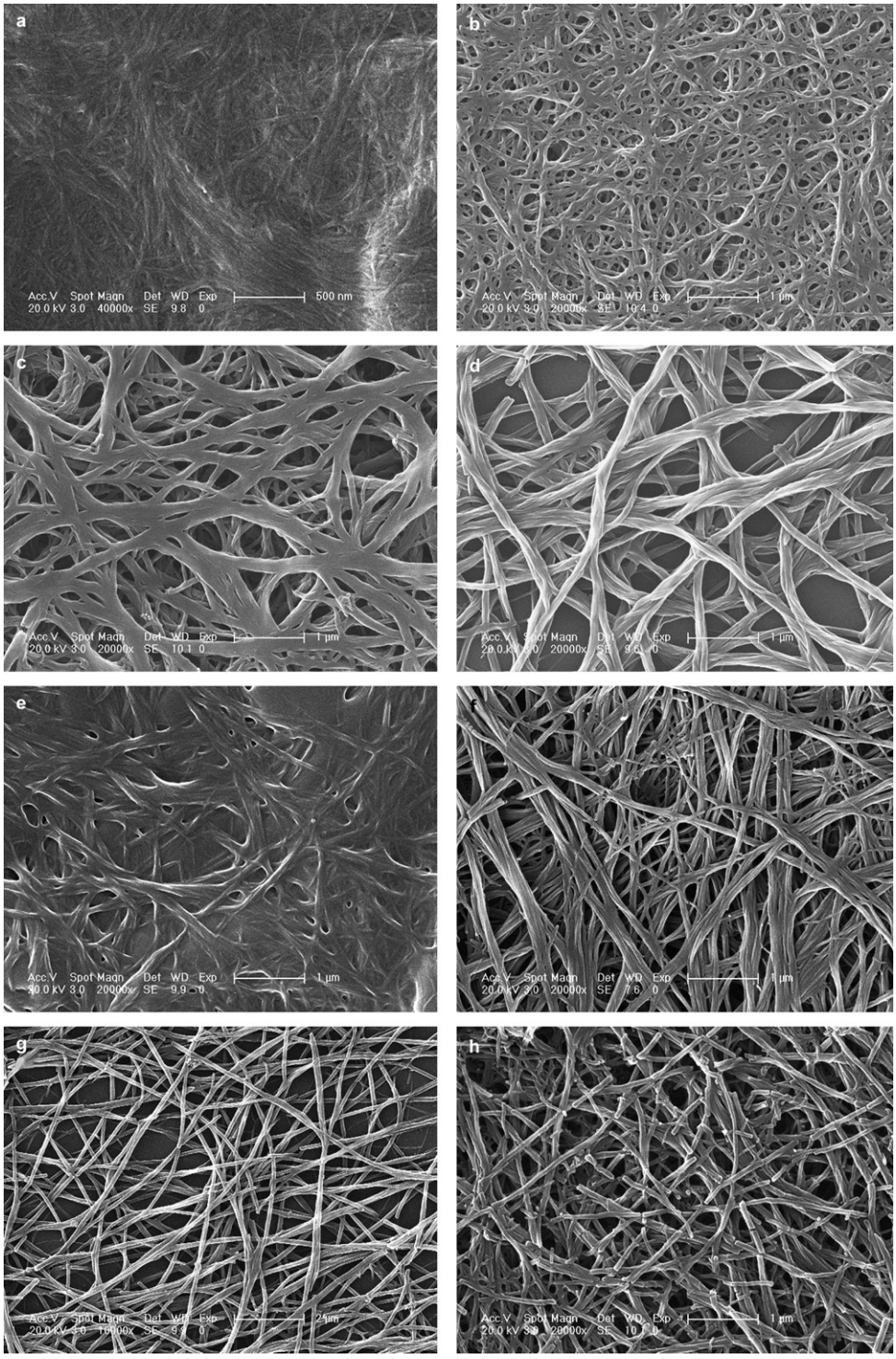

Figure 5. SEM images of the xerogels **2** from chloroform (a), dioxane (b), and THF (c), precipitate **2** in dioxane when cooling slowly (d), xerogel **3** from toluene (e), xerogel **4** from ethyl acetate (f), and xerogel **5** from THF (g) and dioxane (h).

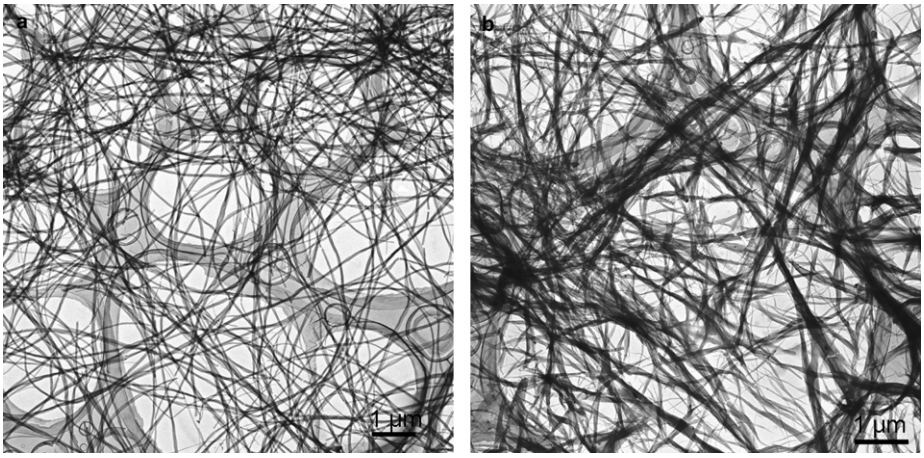

Figure 6. TEM images of gels of **2** from dioxane (a) and THF (b).

(SEM) images of xerogels **2** prepared from chloroform, dioxane, and THF, show a three-dimensional network formed by the entanglement of the nanofibers with a length of several micrometers and a diameter of 30–40 nm, 70–80 nm, and 60–200 nm, respectively (Fig. 5a–c), which is consistent with the gel transparency. In transparent chloroform gel **2**, the diameters of fibers are smaller than those in opaque gels **2** from THF or dioxane. The large diameter of nanofibers may result in the opaqueness of a gel.[16] Interestingly, the precipitate of **2** formed by cooling slowly in dioxane is composed of thicker fibers than gel **2** in dioxane (Fig. 5b and 5d). Slow cooling rate and strong intermolecular hydrogen bonding interaction can together promote further aggregation of 1 D polymeric chains of gelator molecules.

The transmission electronic microscopy (TEM) images of gels **2** in dioxane and THF also demonstrated the existence of a well-developed network structure composed of fibrous aggregates (Fig. 6). The aspect ratios and diameters of the observed fibers by TEM are in accordance with the observations from SEM images. The gels **3**–**5** from different solvents also consist of many nanofibers as confirmed by SEM and TEM. In particular, the nanofibers of gel **5** in THF are longer than those in dioxane, and many fibers in dioxane seem broken, consistent with the observation that the gel in dioxane is easily damaged.

Specific morphologies of the surfaces of xerogel may possess quite different surface wettabilities. Figure 7 displays some pictures of water droplets on glass slides coated with xerogels **2**–**4** from different solvents. The surface wettabilities are strongly dependent on the linker units and gelling solvents.[17] In comparison, the xerogel film of **4** from ethyl acetate gives a hydrophobic surface with a maximum contact angle of 140.7° (Fig. 7e).

2.7. UV–vis and photoluminescence (PL) spectra

The UV–vis absorption spectra of **2**–**5** in gel and dilute solution were measured (Fig. 8). For all compounds in gel, the absorption peaks assigned to the triphenylbenzene display a broader band than those in dilute solution, characteristic of the supramolecular aggregates. It should be noted that for gel **5**, an extra shoulder peak appears at ~325 nm in contrast to dilute solution (Fig. 8d), indicating the existence of some aggregated species.

Figure 9 shows the emission spectra of **2**–**5** in gel and solution at different concentrations. The changes of the fluorescence intensities of **2**–**4** in solution from 2×10^{-6} M to 2×10^{-4} M are typical of aggregation quenching. In particular, the intensity of maximum emission peak of **5** in solution first decreases and then increases in the same concentration range, suggesting that **5** possesses strong self-association ability even in very dilute solution. Moreover, the fluorescence spectra of gels **2**–**5** exhibit several new peaks in the long wavelengths in contrast to those in dilute solution, presumably due to the aggregated species.[18]

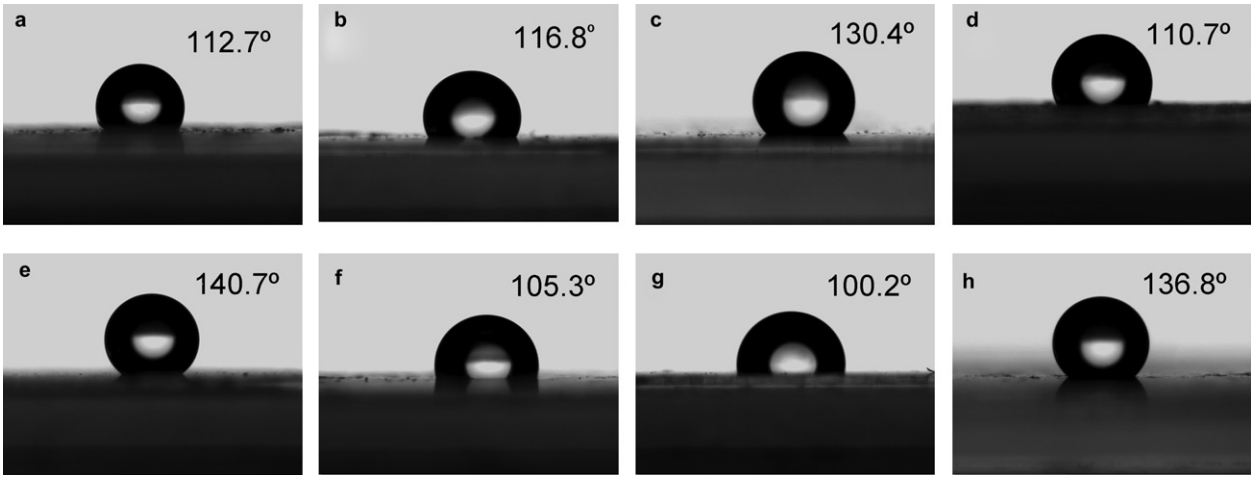

Figure 7. Water droplets on glass slides coated with xerogels **2** from chloroform (a), THF (b), and dioxane (c), xerogels **3** from toluene (d), xerogels **4** from ethyl acetate (e), and toluene (f), and xerogels **5** from THF (g) and dioxane (h).

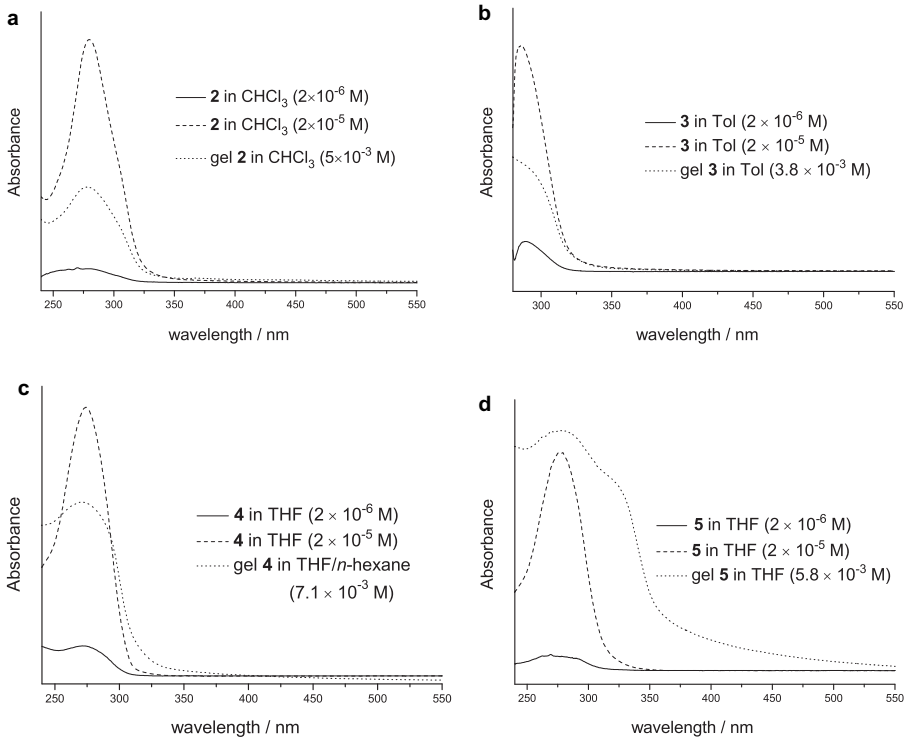

Figure 8. Absorption spectra of **2** in chloroform solution and gel (a), **3** in toluene solution and gel (b), **4** in THF solution and in THF/n-hexane gel (c), and **5** in THF solution and gel (d).

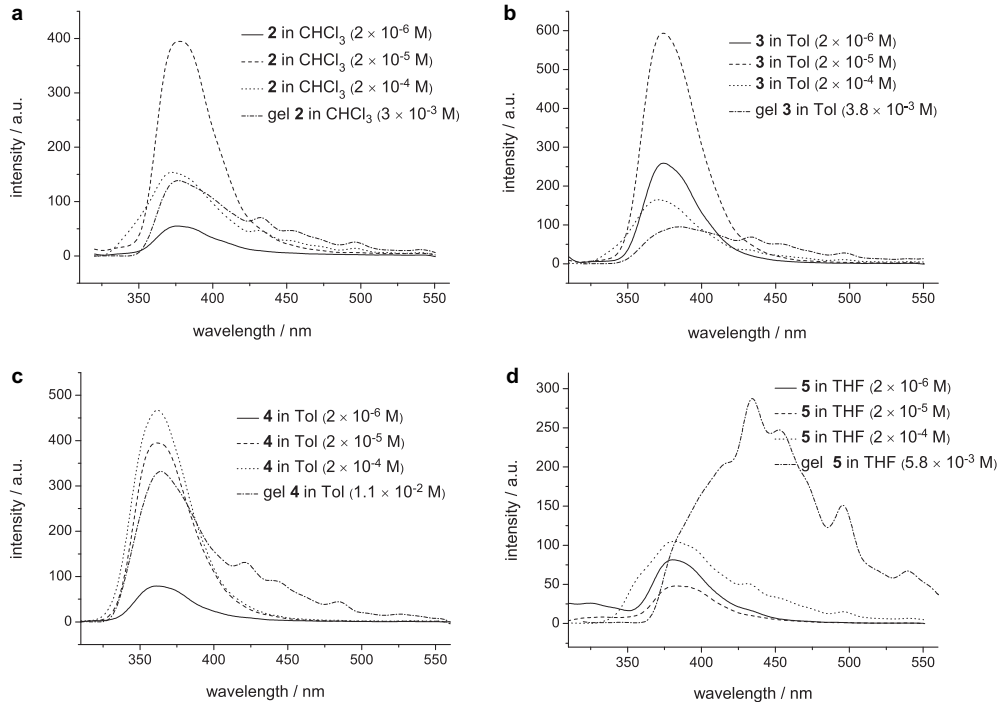

Figure 9. Fluorescence spectra of **2** in chloroform solution and gel (a), **3** in toluene solution and gel (b), **4** in toluene solution and gel (c) and **5** in THF solution and gel (d). λ_{ex}=290 nm.

Interestingly, the maximum emission peak of **5** in gel is red-shifted by ~52 nm in comparison with that in dilute solution, while the maximum emissions of gels **2**–**4** only exhibit the slight shifts. The triphenylbenzene core is not planar due to the steric hindrance and the hydrogen bonding interactions between the linkers. The phenyl ring might rotate to some degree to cope with the formation of the hydrogen bonding.[9] For gels **2**–**4**, the hydrogen bonding between the linkers may be formed flexibly so that a propeller-like conformation of the cores is still favorable. However, a rigid connecting mode (two adjacent hydrogen bonds) between the –CONHNHCO– linkers in gel **5** can promote the cofacial stacking of the cores (Fig. 10). Thus, a better conjugation between the cores results in the red-shift of emission bands.[19]

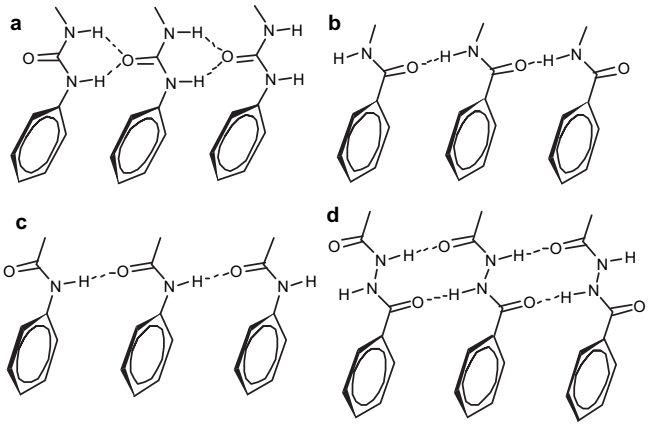

Figure 10. The hydrogen-bonding interactions between urea (a), amide (b and c), and –CONHNHCO– (d) linkers.

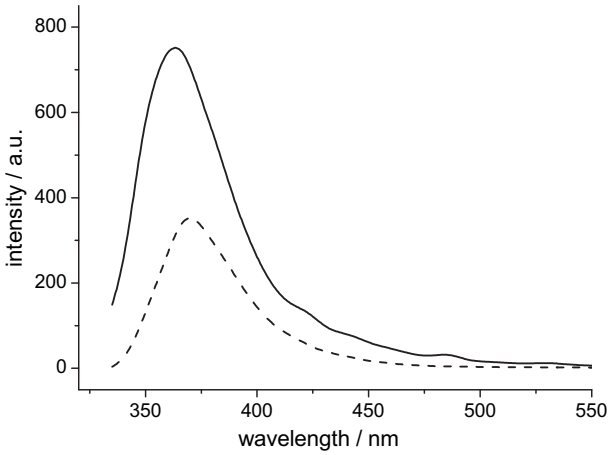

Figure 11. Fluorescence spectra of **4** in THF solution (dash line) and in toluene gel (solid line) at the same concentration (1.1×10^{-2} mol L^{-1}). λ_{ex}=327 nm.

Moreover, a remarkable phenomenon is the fluorescence enhancement of **4** obtained in the gelation (Fig. 11). When excited at 327 nm, gel **4** in toluene exhibits stronger emission than a THF solution of **4** at the same concentration. This is considered as the consequence of aggregation-induced enhanced emission.[20] The gelator molecule in solution is conformationally flexible, which typically renders molecules experience faster non-radiative decay from excited state. Upon formation of gel, however, the resulting ordered aggregates due to intermolecular hydrogen bonding greatly reduce the conformational flexibility and, therefore, slow down the non-radiative decay processes with enhanced fluorescence quantum yields.

2.8. Wide angle X-ray diffraction (WAXD)

In order to study the molecular packing structures of the gel-fibers, WAXD were performed on the xerogels. Generally, the discotic molecules are apt to be arranged into a columnar architecture.[1,3,21] However, Lu et al. previously reported that when alkoxy sidechains of the discotic molecules based on triphenylbenzene become longer or the number of chains is increased, the columnar architecture can be transformed into the lamellar one.[9] As shown in Figure 12, the WAXD patterns of xerogels **2**–**5** reveal a lamellar structure with the interlayer distance of 2.92 nm, 2.49 nm, 2.72 nm, and 2.39 nm, respectively, in the low angle region with the reciprocal spacing ratio of 1:1/2:1/3. These results show that different linker units don't significantly affect the secondary accumulation structure. In addition, the diffractions in wide-angle region give a very broad peak around 20°, attributable to the packing of the alkyl chains by van der Walls interaction.[22]

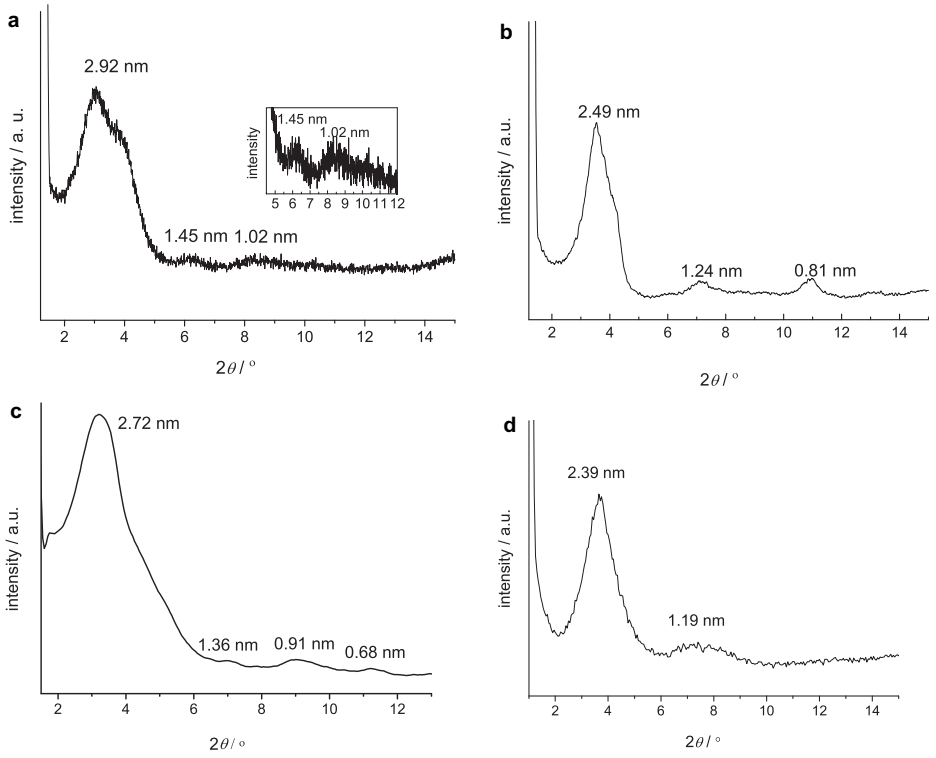

Figure 12. WAXD patterns of xerogels **2** (a), **3** (b), **4** (c), and **5** (d).

2.9. The effect of anion on gel

Considering that the urea moieties are able to bind anion, the effect of anion on gel was assessed. A chloroform gel **2** is transformed into a homogenous solution after the addition of 3 equiv of F^- ions (Fig. 13), while only partial disintegration of the gel is caused on the addition of 1 equiv of F^- ion. However, addition of 3 equiv of other anions, such as I^-, Br^-, Cl^-, BF_4^-, and PF_6^- does not result in the gel-sol phase transition under the same condition. Therefore, gel **2** may be used to selectively recognize F^- ion.

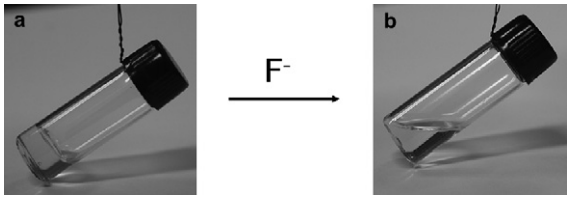

Figure 13. Illustration of the gel-sol phase transition of **2** by the addition of 3 equiv of $(n\text{-}C_4H_9)_4NF$ (TBAF).

The ^1H NMR spectrum of **2** in $CDCl_3$ is also recorded in the presence of 3.0 equiv of F^- ions. The proton signals assigned to urea groups disappear, due to deprotonation by F^- ion according to previous reports.[23] Thus, the intermolecular H-bonding between the urea moieties would be disrupted in the presence of F^- ion, leading to the gel-sol phase transition. This also suggests the importance of hydrogen bonding in the formation of the gel. With increasing amounts of F^- ion, the proton signals attributable to aromatic part shift downfield, indicative of the reduction of intermolecular π–π interactions (Fig. 14).

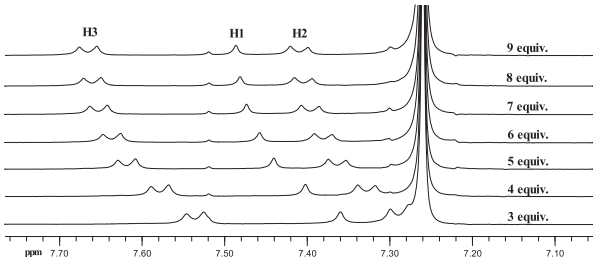

Figure 14. ^1H NMR spectral changes of **2** in $CDCl_3$ at 27 °C upon the addition of 3–9 equiv of TBAF. $c=1.0\times10^{-3}$ mol L^{-1}.

UV–vis and fluorescence spectra are also used to monitor the process. When the gel is completely turned into clear solution on addition of 3 equiv of F^- ions, the maximum absorption peak red-shifts from 277 nm to 292 nm (Fig. 15a), and the fluorescence intensity is weakened. Furthermore, on addition of 3–9 equiv of F^- ions, the maximum emission peak red-shifts from 403 nm to 434 nm (Fig. 15b). These can be well understood as a result of deprotonation of urea groups.

3. Conclusions

In this work, we have described the synthesis and aggregation properties of a family of C_3-symmmetrical discotic molecules tailored with various hydrogen bonding motifs as linkers. The molecular aggregation of **2**–**5** can be promoted by hydrogen bonding interactions between linkers and van der Waals interactions between the hydrophobic alkyl sidechains. However, the π–π stacking between triphenylbenzene cores is not significant. The magnitudes of hydrogen bonding interactions between the triphenylbenzene-centered molecules with approximately identical side chain length are qualitatively in the order of –CONHNHCO–, –NHCONH–>–NHCO–>–CONH–>–NHCSNH–, consequently resulting in different gelation behaviors. The sol-gel transitions of gels **3** and **4** in toluene are thermodynamically reversible, and the formations of gels **2** and **5** in dioxane are kinetically controlled. Slow cooling will lead to the precipitations of **2** and **5**. In gels **2**–**4**, a propeller-like conformation of the triphenylbenzene core is still favorable, but the triphenylbenzene is approximately coplanar in gel **5**. The urea-based gel **2** can selectively recognize F^- ion.

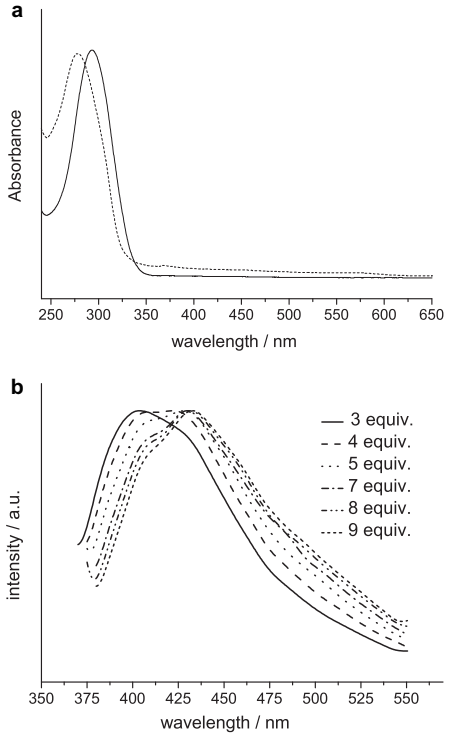

Figure 15. The UV–vis spectra of gel **2** before (dashed line) and after (solid line) addition of 3 equiv of F^- ions (a) and normalized fluoresc-ence spectra of gel **2** after addition of 3–9 equiv of F^- ions (b). $\lambda=360$ nm, $c=3.0\times10^{-3}$ mol L^{-1}.

4. Experimental

4.1. Materials

All reagents and solvents are obtained from commercial supplies and used directly without further purification unless otherwise stated. The solvents for spectroscopic studies are purified according to standard methods.

4.2. Synthesis of the compounds investigated

4.2.1. 1,3,5-Tri(4-(3-dodecylthioureido)phenyl)benzene ***1***. A solution of dodecylisothiocyanate (2.14 g, 9.39 mmol) in dry THF (20 mL) was slowly added to a solution of 1, 3, 5-tris(4-aminophenyl)benzene (1.00 g, 2.85 mmol) in dry THF (30 mL) under nitrogen. The reaction mixture was stirred overnight at room temperature and then refluxed for 5 h. After cooling to room temperature, the solvent was removed under vacuum and the residue was purified by silica column chromatography (dichloromethane/THF=6/1) followed by recrystallization with ethyl acetate to give the off-white solid (1.42 g, 48%). ^1H NMR ($CDCl_3$, 400 MHz) δ (ppm): 7.75 (s, 3H), 7.73 (d, J=8.0 Hz, 6H), 7.70 (s, 3H), 7.33 (d, J=8.0 Hz, 6H), 6.09 (s, 3H), 3.66 (m, 6H), 1.60 (m, 6H), 1.24–1.31 (m, 54H), 0.86 (t, J=8.0 Hz, 9H); ^{13}C NMR ($CDCl_3$, 100 MHz) δ (ppm): 180.48, 141.34, 139.24, 136.04, 128.83, 125.33, 125.01, 45.65, 31.87,

29.60, 29.54, 29.50, 29.30, 29.25, 28.98, 26.90, 22.65, 14.09; FT-IR (KBr, cm^{-1}): 3241, 2923, 2852, 1539, 1512, 1466, 1446, 1316, 1248, 829, 700, 521; MS (ESI) (*m*/*z*) calcd for $C_{63}H_{96}N_6S_3$: 1032.7, found: 1033.1. Anal. Calcd for $C_{63}H_{96}N_6S_3$: C, 73.20; H, 9.36; N, 8.13. Found: C, 73.07; H, 9.39; N, 8.09.

4.2.2. 1,3,5-Tri(4-(3-dodecylureido)phenyl)benzene ***2***. A solution of dodecylisocyanate (2.11 g, 9.96 mmol) in dry THF (20 mL) was slowly added to a solution of 1,3,5-tris(4-aminophenyl)benzene (1.00 g, 2.85 mmol) in dry THF (30 mL). The reaction mixture was stirred overnight at room temperature and then refluxed for 5 h. After cooling to room temperature, the gel-like reaction mixture was concentrated, filtered, and washed with ethyl acetate to give a white waxy solid. Finally, the white solid was dried for 6 h at 60 °C under vacuum (1.03 g, 73%). ^{1}H NMR (DMSO-d_6, 400 MHz, 373 K) δ (ppm): 8.20 (s, 3H), 7.70 (s, 3H), 7.65 (d, *J*=8.4 Hz, 6H), 7.50 (d, *J*=8.4 Hz, 6H), 5.94 (br, 3H), 3.14 (m, 6H), 1.50 (m, 6H), 1.33 (m, 54H), 0.88 (t, *J*=6.4 Hz, 9H); ^{13}C NMR (DMSO-d_6, 100 MHz, 373 K) δ (ppm): 154.70, 140.77, 139.78, 132.70, 126.43, 121.84, 117.79, 38.75, 30.53, 29.11, 28.24, 28.04, 27.87, 25.74, 21.21, 12.91; FT-IR (KBr, cm^{-1}): 3323, 2922, 2852, 1643, 1588, 1555, 1528, 1234, 1069, 833, 653, 526; MS (ESI) (*m*/*z*) calcd for $C_{63}H_{96}N_6O_3$: 984.8, found: 985.2. Anal. Calcd for $C_{63}H_{96}N_6O_3$: C, 76.78; H, 9.82; N, 8.53. Found: C, 76.67; H, 9.89; N, 8.49.

4.2.3. 1,3,5-Tri(4-dodecanamidophenyl)benzene ***3***. Dodecanoyl chloride (1.40 g, 6.40 mmol) was dissolved in dry THF (10 mL), and the solution was added dropwise to dry THF (15 mL) solution consisting of 1,3,5-tris(4-aminophenyl)-benzene (0.5 g, 1.42 mmol) and triethylamine (1.20 mL, 8.54 mmol) at 0 °C. After stirring at room temperature for 24 h, the reaction mixture was purified by silica gel column chromatography (dichloromethane/THF=1/1) to give pure white product (0.87 g, 65%). ^{1}H NMR ($CDCl_3$, 400 MHz) δ (ppm): 7.65 (s, 3H), 7.61 (s, 12H), 7.26 (s, 3H), 2.39 (t, *J*=8.0 Hz, 6H), 1.75 (m, 6H), 1.26–1.40 (m, 48H), 0.88 (t, *J*=8.0 Hz, 9H); ^{13}C NMR (DMSO-d_6, 150 MHz) δ (ppm): 171.28, 141.02, 139.01, 134.57, 127.21, 122.87, 119.27, 36.42, 31.25, 28.98, 28.95, 28.89, 28.75, 28.67, 28.63, 25.06, 22.05, 13.89; FT-IR (KBr, cm^{-1}): 3292, 2923, 2852, 1660, 1599, 1524, 825, 527; MS (ESI) (*m*/*z*) calcd for $C_{60}H_{87}N_3O_3$: 897.7, found: 898.1. Anal. Calcd for $C_{60}H_{87}N_3O_3$: C, 80.22; H, 9.76; N, 4.68. Found: C, 80.35; H, 9.59; N, 4.62.

4.2.4. 1,3,5-Tri(4-dodecylcarbamoylphenyl)benzene ***4***. 1,3,5-Tri-(*p*-carbonylphenyl)benzene (0.60 g, 1.14 mmol) in $SOCl_2$ (30 mL) was refluxed overnight and excess $SOCl_2$ was removed. The resulting carbonyl chloride was dissolved in dry THF (50 mL). Then, a solution consisting of dodecan-1-amine (1.02 g, 5.47 mmol) and triethylamine (1.20 mL, 8.21 mmol) in dry THF (20 mL) was added dropwise. The reaction mixture was stirred overnight. The product was purified by silica gel column chromatography (CH_2Cl_2/EtOAc=1/1) (0.86 g, 67%). ^{1}H NMR ($CDCl_3$, 400 MHz) δ (ppm): 7.81 (d, *J*=8.0 Hz, 6H), 7.65 (s, 3H), 7.59 (d, *J*=8.0 Hz, 6H), 6.48 (br, 3H), 3.48 (m, 6H), 1.65 (m, 6H), 1.26–1.40 (m, 54H), 0.88 (t, *J*=6.8 Hz, 9H); ^{13}C NMR ($CDCl_3$, 100 MHz) δ (ppm): 167.17, 143.28, 141.38, 134.05, 127.54, 127.20, 125.44, 40.24, 31.89, 29.68, 29.60, 29.33, 27.06, 22.66, 14.08; FT-IR (KBr, cm^{-1}): 3299, 2924, 2852, 1636, 1545, 1505, 1466, 1438, 1314, 845, 767, 694; MS (ESI) (*m*/*z*) calcd for $C_{63}H_{93}N_3O_3$: 939.7, found: 940.2. Anal. Calcd for $C_{63}H_{93}N_3O_3$: C, 80.46; H, 9.97; N, 4.47. Found: C, 80.53; H, 10.05; N, 4.40.

4.2.5. 1,3,5-Tri(4-dodecanamidocarbamoylphenyl)benzene ***5***. Compound **5** was synthesized as described for **4**. ^{1}H NMR (DMSO-d_6, 400 MHz) δ (ppm): 10.38 (s, 3H), 9.85 (s, 3H), 8.11 (s, 3H), 8.09 (d, *J*=8.0 Hz, 6H), 8.03 (d, *J*=8.0 Hz, 6H), 2.20 (m, 6H), 1.57 (m, 6H), 1.27 (m, 48H), 0.86 (t, *J*=6.4 Hz, 9H); ^{13}C NMR (DMSO-d_6, 100 MHz) δ (ppm): 171.58, 165.04, 142.78, 140.67, 131.66, 128.02, 127.21, 125.25, 33.31, 31.28, 29.01, 28.80, 28.70, 28.57, 25.08, 22.07, 13.92; FT-IR (KBr, cm^{-1}): 3205, 2955, 2922, 2853, 1601, 1562, 1471, 1070, 956, 843; MS (ESI) (*m*/*z*) calcd for $C_{63}H_{90}N_6O_6$: 1026.7, found: 1027.2. Anal. Calcd for $C_{63}H_{90}N_6O_6$: C, 73.65; H, 8.83; N, 8.18. Found: C, 73.70; H, 8.79; N, 8.25.

4.2.6. 1,3,5-Tri(3-dodecylcarbamoylphenyl)benzene ***6***. 1,3,5-Tri-(*m*-carbonylphenyl)benzene (0.50 g, 1.14 mmol) in $SOCl_2$ (30 mL) was refluxed overnight and excess $SOCl_2$ was removed in vacuo. The obtained carbonyl chloride was dissolved in dry THF (40 mL). Then a solution containing dodecan-1-amine (0.85 g, 4.56 mmol) and triethylamine (0.95 mL, 6.84 mmol) was added dropwise at 0 °C. After the reaction mixture was stirred for 24 h at room temperature, the solvent was evaporated under vacuum and the residue was purified by silica gel chromatography (CH_2Cl_2/EtOAc=10/1) to give pure white solid (0.95 g, 89%). ^{1}H NMR ($CDCl_3$, 400 MHz) δ (ppm): 8.06 (s, 3H), 7.77 (s, 3H), 7.74 (m, 6H), 7.51 (t, *J*=7.6 Hz, 3H), 6.37 (br, 3H), 3.48 (m, 6H), 1.66 (m, 6H), 1.25–1.38 (m, 54H), 0.87 (t, *J*=6.8 Hz, 9H); ^{13}C NMR ($CDCl_3$, 100 MHz) δ (ppm):167.50, 141.59, 141.04, 135.44, 130.12, 128.99, 125.96, 125.43, 40.31, 31.89, 29.61, 29.34, 27.07, 22.66, 14.09; FT-IR (KBr, cm^{-1}): 3290, 2956, 2921, 2851, 1631, 1541, 1468, 1327, 869, 811, 698; MS (ESI) (*m*/*z*) calcd for $C_{63}H_{93}N_3O_3$: 939.7, found: 940.3. Anal. Calcd for $C_{63}H_{93}N_3O_3$: C, 80.46; H, 9.97; N, 4.47. Found: C, 80.43; H, 10.03; N, 4.39.

4.2.7. 1,3,5-Tri(4-aminophenyl)benzene ***7***. Tetrachloride silicon (20 mL, 0.18 mol) was added dropwise to a solution of *p*-nitroacetophenone (10.00 g, 0.06 mol) in absolute ethanol (60 mL) at 0 °C. A yellow precipitate was formed immediately and then the reaction mixture was refluxed for 10 h. After cooled to room temperature, the mixture was poured to ice-water and stirred for 10 min. The resulting yellow precipitate was filtered and dried, and added to ethanol (200 mL) directly with Pd/C (0.8 g), which was heated to reflux. Then $NH_2NH_2 \cdot H_2O$ (80%, 25 mL) was added dropwise to the hot solution. After refluxing for 10 h, the precipitate was taken off by filtration and the solution was cooled to room temperature, and the white precipitate was collected. The solid was recrystallized in ethanol and dried under vacuum. ^{1}H NMR (DMSO-d_6, 400 MHz) δ (ppm): 7.48 (s, 3H), 7.47 (d, *J*=8.8 Hz, 6H), 6.66 (d, *J*=8.8 Hz, 6H), 5.22 (s, 6H); ^{13}C NMR (DMSO-d_6, 150 MHz) δ (ppm): 148.31, 141.57, 128.06, 127.42, 120.37, 114.18; FT-IR (KBr, cm^{-1}): 3434, 3355, 3210, 3028, 1621, 1607, 1515, 1280, 1177, 829; MS (ESI) (*m*/*z*) calcd for $C_{24}H_{21}N_3$: 351.2, found: 351.5.

4.2.8. 1,3,5-Tri(p-carboxyphenyl)benzene ***8***. To a mixture of 1,3,5-tribromobenzene (5.0 g, 15.88 mmol), *p*-methoxy-carbonylphenyl boronic acid (11.43 g, 63.53 mmol), Na_2CO_3 (8.42 g, 79.41 mmol), and $Pd(PPh_3)_4$ (1.38 g, 1.19 mmol) were added degassed toluene–methanol–water (80/40/40 mL) under an argon atmosphere. The resulting reaction mixture was stirred for 48 h under reflux. After removal of the solvent, the residue was extracted with dichloromethane (80×3 mL), washed with brine (80 mL), dried over anhydrous $MgSO_4$ and concentrated in vacuo. The residue was purified by silica gel column chromatography (petroleum ether/dichloromethane=1/5) to give 1,3,5-tri(*p*-methoxycarbonylphenyl)benzene (5.41 g, 71%), which was hydrolyzed with 6 M NaOH to afford the title compound. ^{1}H NMR (DMSO-d_6, 400 MHz) δ (ppm): 13.04 (s, 3H), 8.10 (s, 3H), 8.06 (s, 12H); ^{13}C NMR (DMSO-d_6, 150 MHz) δ (ppm): 167.11, 143.81, 140.72, 130.02, 129.88, 127.39, 125.54; FT-IR (KBr, cm^{-1}): 3382, 3014, 2660, 2538, 1697, 1608, 1569, 1512, 1447, 1416, 1393, 1317, 1286, 1241, 1181, 1016, 847, 764; MS (ESI) (*m*/*z*) calcd for $C_{27}H_{18}O_6$: 438.1, found: 438.6.

4.2.9. 1,3,5-Tri(m-carboxyphenyl)benzene ***9***. Compound **9** was synthesized as described for **8**. ^{1}H NMR (DMSO-d_6, 400 MHz) δ (ppm): 13.12 (s, 3H), 8.36 (s, 3H), 8.17 (d, *J*=7.6 Hz, 3H), 8.01 (d, *J*=7.6 Hz,

3H), 7.99 (s, 3H), 7.66 (t, J=7.6 Hz, 3H); ^{13}C NMR (DMSO-d_6, 150 MHz) δ (ppm): 167.24, 141.07, 140.19, 131.77, 131.55, 129.31, 128.64, 127.78, 125.00; FT-IR (KBr, cm^{-1}): 3005, 2889, 2649, 2560, 1702, 1606, 1582, 1486, 1426, 1394, 1302, 1272, 1239, 750, 687, 672; MS (ESI) (m/z) calcd for $C_{27}H_{18}O_6$: 438.1, found: 438.4.

4.3. Preparation of the gels

The gels were prepared by heating the organogelator and the solvent in a vial (35×15 mm) until the complete dissolution of the solid. After the solution is allowed to stand at room temperature (25±5 °C) for 30 min, the state of the mixture is evaluated by the 'stable to inversion of test tube' method.

4.4. Measurements

^{1}H NMR and ^{13}C NMR spectra are recorded on Bruker AV400 or AV600 spectrometer at 300 K unless otherwise stated. Chemical shifts are reported downfield with TMS (δ=0.00 ppm) as the standard. For ^{13}C NMR spectra, chemical shifts are reported on the scale relative to deuterated solvent as internal standard ($CDCl_3$, δ=77.00 ppm, DMSO-d_6, δ=39.50 ppm). The coupling constants are reported in hertz. Mass spectra (ESIMS) are recorded with a Thermo Finnigan LCQ instrument. IR spectra for the samples of xerogels and in THF solutions are performed on a Bio-Rad FTS135 infrared spectrometer at room temperature. Elemental analyses (C, H, N) are carried out with a VarioEL instrument. For differential scanning calorimetry measurements, a DSC Q100 TA instrument is used. UV–vis spectra are recorded on an UV-2500 UV–vis spectrophotometer at room temperature. The fluorescent spectra are recorded on Perkin–Elmer LS 50B fluorescence spectrophotometer at room temperature. TEM is performed on a JEOL JEM-1011 transmission electron microscope operated at an acceleration voltage of 100 kV. Samples are prepared by wiping a small amount of gel samples onto carbon-coated copper grid followed by naturally evaporating the solvent. SEM pictures are taken using an XL 30 ESEM FEG field emission scanning electron microscope with 20 kV operating voltage. PXRD patterns are recorded by PW1710 BASED X-ray diffractometer with CuKα1 radiation source. CA measurements are performed using the sessile drop method (Dataphysics, OCA 20). The water droplets are introduced using a microsyringe, and images are captured to measure the angle of the liquid-solid interface. Each sample is recorded at three different points. Chromatographic purification is conducted using 100–200 mesh silica gel.

Acknowledgements

The work is supported by the National Natural Science Fundation of China (20502024) and Free Exploration Project of Innovation III of Changchun Institute of Applied Chemistry (CX07QZJC-02).

Supplementary data

Supplementary data associated with this article can be found in the online version, at doi:10.1016/j.tet.2010.02.094.

References and notes

1. (a) Smulders, M. M. J.; Schenning, A. P. H. J.; Meijer, E. W. *J. Am.Chem. Soc.* **2007**, *130*, 606; (b) Smulders, M. M. J.; Buffeteau, T.; Cavagnat, D.; Wolffs, M.; Schenning, A. P. H. J.; Meijer, E. W. *Chirality* **2008**, *20*, 1016; (c) Ollvler, C.; Solarl, E.; Scopelltl, R.; Severln, K. *Inorg. Chem.* **2008**, *47*, 4454; (d) Martín-Rapún, R.; Byelov, D.; Palmans, A. R. A.; de Jeu, W. H.; Meijer, E. W. *Langmuir* **2009**, *25*, 8794; (e) van Herrikhuyzen, J.; Jonkheijm, P.; Schenning, A. P. H. J.; Meijer, E. W. *Org. Biomol. Chem.* **2006**, *4*, 1539; (f) Castaldi, M. P.; Gibson, S. E.; Rudd, M.; White, A. J. P. *Chem.—Eur. J.* **2006**, *12*, 138; (g) Hennrich, G.; Ortiz, P. D.; Cavero, E.; Hanes, R. E.; Serrano, J. L. *Eur. J. Org. Chem.* **2008**, 4575; (h) Benincori, T.; Marchesi, A.; Mussini, P. R.; Pilati, T.; Ponti, A.; Rizzo, S.; Sannicolò, F. *Chem.—Eur. J.* **2009**, *15*, 86; (i) Feng, X.; Pisula, W.; Zhi, L.; Takase, M.; Müllen, K. *Angew. Chem., Int. Ed.* **2008**, *47*, 1703; (j) Schnopp, M.; Haberhauer, G. *Eur. J. Org. Chem.* **2009**, 4458; (k) Castaldi, M. P.; Gibson, S. E.; Rudd, M.; White, A. J. P. *Angew. Chem., Int. Ed.* **2005**, *44*, 3432; (l) Wang, J. Y.; Yan, J.; Ding, L.; Ma, Y.; Pei, J. *Adv. Funct. Mater.* **2009**, *19*, 1746; (m) Angiolini, L.; Benelli, T.; Giorgini, L. *Chirality*. doi:10.1002/chir.20712; (n) Pintér, Á.; Haberhauer, G. *Chem.—Eur. J.* **2008**, *14*, 11061; (o) Garcí-Frutos, E. M.; Gómez-Lor, B.; Monge, Á.; Gutiérrez-Puebla, E.; Alkorta, I.; Elguero, J. *Chem.—Eur. J.* **2008**, *14*, 8555; (p) Kotha, S.; Kashinath, D.; Lahiri, K.; Sunoj, R. B. *Eur. J. Org. Chem.* **2004**, 4003; (q) Treossi, E.; Liscio, A.; Feng, X.; Palermo, V.; Müllen, K.; Samorì, P. *Small* **2009**, *5*, 112; (r) van den Hout, K. P.; Martín-Rapún, R.; Vekemans, J. A. J. M.; Meijer, E. W. *Chem.—Eur. J.* **2007**, *13*, 8111; (s) Palmans, A. R. A.; Vekemans, J. A. J. M.; Havinga, E. E.; Meijer, E. W. *Angew. Chem., Int. Ed.* **2003**, *36*, 2648; (t) Reza, A. F. G. M.; Higashibayashi, S.; Sakurai, H. *Chem. Asian. J.* **2009**, *4*, 1329.
2. van Hameren, R.; Schön, P.; van Buul, A. M.; Hoogboom, J.; Lazarenko, S. V.; Gerritsen, J. W.; Engelkamp, H.; Christianen, P. C. M.; Heus, H. A.; Maan, J. C.; Rasing, T.; Speller, S.; Rowan, A. E.; Elemans, J. A. A. W.; Nolte, R. J. M. *Science* **2006**, *314*, 1433.
3. (a) de Loos, M.; Feringa, B. L.; van Esch, J. H. *Eur. J. Org. Chem.* **2005**, 3615; (b) Hoeben, F. J. M.; Jonkheijm, P.; Meijer, E. W.; Schenning, A. P. H. J. *Chem. Rev.* **2005**, *105*, 1491; (c) Sangeetha, N. M.; Maitra, U. *Chem. Soc. Rev.* **2005**, *34*, 821; (d) Abdallah, D. J.; Weiss, R. G. *Adv. Mater.* **2000**, *12*, 1237; (e) Guenet, J.-M. *Macromol. Symp.* **2006**, *241*, 45.
4. Zhou, Y.; Xu, M.; Yi, T.; Xiao, S.; Zhou, Z.; Li, F.; Huang, C. *Langmuir* **2007**, *23*, 202.
5. Govindaraji, S.; Nakache, P.; Marks, V.; Pomerantz, Z.; Zaban, A.; Lellouche, J. P. *J. Org. Chem.* **2006**, *71*, 9139.
6. Danila, I.; Riobé, F.; Puigmartí-Luis, J.; del Pino, Á. P.; Wallis, J. D.; Amabilino, D. B.; Avarvari, N. *J. Mater. Chem.* **2009**, *19*, 4495.
7. van Gorp, J. J.; Vekemans, J. A. J. M.; Meijer, E. W. *J. Am. Chem. Soc.* **2002**, *124*, 14759.
8. Shi, N.; Yin, G.; Li, H.; Han, M.; Xu, Z. *New J. Chem.* **2008**, *32*, 2011.
9. Bao, C.; Lu, R.; Jin, M.; Xue, P.; Tan, C.; Xu, T.; Liu, G.; Zhao, Y. *Chem.—Eur. J.* **2006**, *12*, 3287.
10. de Loos, M.; van Esch, J. H.; Kellogg, R. M.; Feringa, B. L. *Tetrahedron* **2007**, *63*, 7285.
11. Yamanaka, M.; Nakagawa, T.; Aoyama, R.; Nakamura, T. *Tetrahedron* **2008**, *64*, 11558.
12. Chen, Y.; Zhu, B.; Zhang, F.; Han, Y.; Bo, Z. *Angew. Chem., Int. Ed.* **2008**, *47*, 6015.
13. Suzuki, M.; Sato, T.; Shirai, H.; Hanabusa, K. *New J. Chem.* **2006**, *30*, 1184.
14. (a) George, M.; Tan, G.; John, V. T.; Weiss, R. G. *Chem.—Eur. J.* **2005**, *11*, 3243; (b) Wurthner, F.; Hanke, B.; Lysetska, M.; Lambright, G.; Harms, G. S. *Org. Lett.* **2005**, *7*, 967; (c) Suzuki, M.; Nakajima, Y.; Yumoto, M.; Kimura, M.; Shirai, H.; Hanabusa, K. *Langmuir* **2003**, *19*, 8622.
15. (a) Suzuki, M.; Nigawara, T.; Yumoto, M.; Kimura, M.; Shirai, H.; Hanabusa, K. *Tetrahedron Lett.* **2003**, *44*, 6841; (b) Velázquez, D. G.; Díaz, D. D.; Ravelo, Á. G.; Marrero-Tellado, J. J. *Eur. J. Org. Chem.* **2007**, 1841; (c) Qu, S.; Li, M. *Tetrahedron* **2008**, *64*, 10890; (d) Xin, H.; Wang, H.; Bai, B.; Pang, D.; Li, M. *J. Mol. Liq.* **2008**, *139*, 143.
16. Xing, B.; Choi, M.-F.; Xu, B. *Chem.—Eur. J.* **2002**, *8*, 5028.
17. Zhou, Y.; Yi, T.; Li, T.; Zhou, Z.; Li, F.; Huang, W.; Huang, C. *Chem. Mater.* **2006**, *18*, 2974.
18. Hisaki, I.; Shigemitsu, H.; Sakamoto, Y.; Hasegawa, Y.; Okajima, Y.; Nakano, K.; Tohnai, N.; Miyata, M. *Angew. Chem., Int. Ed.* **2009**, *48*, 5465.
19. (a) An, B.-K.; Kwon, S.-K.; Jung, S.-D.; Park, S. Y. *J. Am. Chem. Soc.* **2002**, *124*, 14410; (b) An, B.-K.; Lee, D.-S.; Lee, J.-S.; Park, Y.-S.; Song, H.-S.; Park, S. Y. *J. Am. Chem. Soc.* **2004**, *126*, 10232; (c) Luo, J.; Xie, Z.; Lam, J. W. Y.; Cheng, L.; Chen, H.; Qiu, C.; Kwok, H. S.; Zhan, X.; Liu, Y.; Zhu, D.; Tang, B. Z. *Chem. Commun.* **2001**, 1740.
20. (a) Shen, Y.-T.; Li, C.-H.; Chang, K.-C.; Chin, S.-Y.; Lin, H.-A.; Liu, Y.-M.; Hung, C.-Y.; Hsu, H.-F.; Sun, S.-S. *Langmuir* **2009**, *25*, 8714; (b) Kim, T. H.; Choi, M. S.; Sohn, B.-H.; Park, S.-Y.; Lyoo, W. S.; Lee, T. S. *Chem. Commun.* **2008**, 2364; (c) Leong, W. L.; Tam, A. Y.-Y.; Batabyal, S. K.; Koh, L. W.; Kasapis, S.; Yam, V. W.-W.; Vittal, J. J. *Chem. Commun.* **2008**, 3628.
21. (a) Shitakawa, M.; Kdwdno, S.; Fujita, N.; Sada, K.; Shinkai, S. *J. Org. Chem.* **2003**, *68*, 5037; (b) Kadam, J.; Faul, C. F. J.; Scherf, U. *Chem. Mater.* **2004**, *16*, 3867.
22. Tsou, C.-C.; Sun, S.-S. *Org. Lett.* **2006**, *8*, 387.
23. (a) Yamanaka, M.; Nakamura, T.; Nakagawa, T.; Itagaki, H. *Tetrahedron Lett.* **2007**, *48*, 8990; (b) Wang, C.; Zhang, D.; Zhu, D. *Langmuir* **2007**, *23*, 1478; (c) Varghese, R.; George, S. J.; Ajayaghosh, A. *Chem. Commun.* **2005**, 593.